Extremely high thermal conductivity of graphene: Prospects for thermal management applications in nanoelectronic circuits

S. Ghosh,[1] I. Calizo,[1] D. Teweldebrhan,[1] E. P. Pokatilov,[1,a)] D. L. Nika,[1,a)] A. A. Balandin,[1,b)] W. Bao,[2] F. Miao,[2] and C. N. Lau[2]
[1]*Nano-Device Laboratory, Department of Electrical Engineering, University of California-Riverside, Riverside, California 92521, USA*
[2]*Department of Physics and Astronomy, University of California-Riverside, Riverside, California 92521 USA*

(Received 26 February 2008; accepted 18 March 2008; published online 16 April 2008)

The authors reported on investigation of the thermal conductivity of graphene suspended across trenches in Si/SiO_2 wafer. The measurements were performed using a noncontact technique based on micro-Raman spectroscopy. The amount of power dissipated in graphene and corresponding temperature rise were determined from the spectral position and integrated intensity of graphene's G mode. The extremely high thermal conductivity in the range of ~3080–5150 W/m K and phonon mean free path of ~775 nm near room temperature were extracted for a set of graphene flakes. The obtained results suggest graphene's applications as thermal management material in future nanoelectronic circuits. © *2008 American Institute of Physics*. [DOI: 10.1063/1.2907977]

As the electronic industry moves toward nanometer designs, one of the most important challenges is growing chip power consumption. Thus, thermal management in electronic circuits is becoming an integral part of the design.[1] As the performance of ultralarge scale integrated (ULSI) circuits depends on temperature T, even a small increase in T results in reduction of the device lifetime. A possible approach for solving the thermal problem is finding a material with extremely high thermal conductivity K, which can be integrated with Si complementary metal-oxide semiconductor (CMOS) technology. Diamond and carbon nanotubes (CNTs) have been considered for such applications.[2,3] Although these materials have high thermal conductivity[4–6] they are not well suited for integration with CMOS.

In this letter, we show that graphene, i.e., individual sheets of sp^2-hybridized carbon bound in two dimensions,[7–9] exhibits an extremely high thermal conductivity and long phonon mean free paths (MFP). The letter provides details of a measurement technique and explains the obtained K values with a simple model. A large number of graphene layers have been produced by the mechanical exfoliation of bulk highly oriented pyrolitic graphite (HOPG) using the standard technique.[7–10] We used Si/SiO_2 substrates with an array of trenches fabricated by the reactive ion etching (RIE). The nominal depth of the RIE trenches was ~300 nm, while the trench width D varied in the range of 1–5 μm. Among the samples, we selected long graphene flakes with a relatively constant width W suspended over the trenches and connected through the few-layer graphene regions to large graphitic pieces at the distance of few micrometers from the trench edges. The suspended single-layer graphene (SLG) flakes were found with the help of Raman spectroscopy.[11–14] The large graphitic pieces connected to SLG acted as heat sinks.

None of the conventional techniques for measuring thermal conductivity of material worked well for the atomically thick graphene layers. For this reason, we developed an approach on the basis of confocal micro-Raman spectroscopy. The schematic of the experiment and samples are shown in Fig. 1. The laser light is focused in the middle of the suspended SLG with the spot size of about ~1 μm.[15] A fraction of the excitation light (λ=488 nm) is absorbed by graphene, which results in the heating power P_G, while the remaining light is absorbed by the trench. Since K of the air is negligible, the heat generated in graphene laterally propagates through the layer with the thickness of $a_G = 0.35 \pm 0.01$ nm toward the heat sinks on the sides of the flakes. Due to the small cross-sectional area of the heat conducting channel, even a small power dissipated in graphene can lead to a detectable rise of the local temperature.[16]

The suspended portion of graphene is essential for (i) forming a nearly plane heat wave front, which propagates to the heat sinks, (ii) reducing graphene—substrate coupling, and (iii) determining the fraction of power dissipated in SLG via the original procedure outlined below. The temperature rise ΔT_G in the middle of the suspended portion of graphene can be established by measuring the shift in position of the graphene G peak $\Delta\omega$ and using the peak temperature coefficient χ_G, which we reported earlier.[16,17] In this case, the micro-Raman spectrometer acts as a thermometer, which gives $\Delta T_G = \Delta\omega/\chi_G$. We induced substantial heating in the

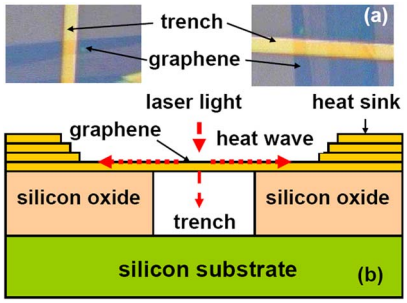

FIG. 1. (Color online) (a) High-resolution scanning electron microscopy image of the suspended graphene flakes. (b) Schematic of the experimental setup for measuring the thermal conductivity of graphene.

a)On leave from: the Department of Theoretical Physics, Moldova State University, Chisinau, Republic of Moldova.
b)Author to whom correspondence should be addressed. Electronic mail: balandin@ee.ucr.edu. URL: http://ndl.ee.ucr.edu.

middle of the suspended portion of the graphene flake. The average temperature rise along the length of the about flake was about ~70–100 K.

The heat transport in graphene layer in our experiment is at least partially diffusive. The latter is expected from the phonon MFP data reported for a rather similar material system such as suspended CNTs.[5,6,18,19] It was found that MFP in CNTs is ~250–750 nm at RT.[18] In our setup, the distance from the trench edge to the sink was in the range of 6–10 μm. For the plane-wave heat front propagating in two opposite directions from the middle of SLG, we can write $K=(L/2a_GW)(\Delta P_G/\Delta T_G)$. Here, ΔT_G is the change in the temperature in the suspended portion of graphene flake due to the change in the power ΔP_G dissipated in graphene. Finally, the thermal conductivity can be determined as

$$K=(L/2a_GW)\chi_G(\Delta\omega/\Delta P_G)^{-1}. \quad (1)$$

It is not possible to directly measure ΔP_G. The detector placed at the site of the sample measures $P_D=P_G+P_S$, where P_S is the power loss in Si trench. To determine P_G, we developed a calibration procedure with HOPG used for exfoliation of graphene. The power absorbed in SLG can be written as $P_G=\alpha_G a_G(1+R_{Si})I_0A$, where A is the illuminated area, I_0 is the laser intensity on the surface, α_G is the absorption coefficient in graphene, and R_{Si} is the reflection coefficient of Si. Here, we took into account the power, which is reflected from the Si trench and absorbed by the suspended portion of graphene. The reflection from SLG is assumed negligible, which is in line with the findings of Ref. 20. The integrated Raman intensity from SLG is given as[21] $\Delta I_G=N\sigma_G I_0$, where N is the number of the scattering atoms in the surface area A and σ_G is the Raman scattering cross section. Now we can relate the integrated Raman intensity to the absorbed power as $\Delta I_G=(N/A)(\sigma_G/\alpha_G a_G)P_G/(1+R_{Si})$.

Focusing the same laser beam on the calibration HOPG, we set $P_D=I_0A$. The integrated Raman scattered intensity from HOPG is obtained by summation over all n graphene layers, which make up HOPG, i.e., $\Delta I_{HOPG}=N\sigma_H I_0\Sigma_{n=1}^{\infty}\exp(-2\alpha_H a_H n)$, where α_H is the absorption coefficient and a_H is the thickness of each monolayer. The later leads to $\Delta I_{HOPG}=(1/2)(N/A)(\sigma_H/\alpha_H a_H)P_D(1-R_H)$, where R_H is the reflection coefficient for HOPG. Defining the ratio of the integrated intensities as $\varsigma=\Delta I_G/\Delta I_{HOPG}$, we express the power absorbed in graphene through the power measured by the detector as

$$P_G=(\varsigma/2)[\sigma_H\alpha_G a_G/\sigma_G\alpha_H a_H](1+R_{Si})(1-R_H)P_D. \quad (2)$$

Since the term in the square brackets is about unity, the measurement of ς completes the calibration. Figure 2 shows measured ΔI_G and ΔI_{HOPG} for a typical suspended graphene and its "native" HOPG. The measured intensities define ς, which is almost constant over the examined ΔP_D range. Using the characteristic values of $R_H=0.27–0.34$ (Ref. 22) and $R_{Si}=0.25–0.30$ for the rough Si trench together with the measured ς, we obtain that $P_G\approx(0.11–0.12)P_D$. Although the larger fraction of laser power is lost in the trench, it does not interfere with the measurement because the heat in Si trench diffuses to the substrate bottom and does not form a parallel conduction channel to the graphitic heat sinks.

We independently confirm that substantial amount of power is dissipated in the trench by measuring the shift of Si 522 cm^{-1} peak with the laser excitation power. The temperature coefficient, defined as $\Delta\omega_\Gamma(T)/T\omega_\Gamma(T=0)$, for Si is well known and reported to be in the range of $\sim -4.7\times10^{-5}$ (Ref. 23) $-1–5.4\times10^{-5}/°C$.[24] From the measured shift of $\Delta\omega\sim1$ cm^{-1}, we estimated that the temperature rise in Si trench is $\Delta T\sim35$ K. The significant rise despite a large thermal conductivity of Si (~145 W/m K at RT) is in line with our assessment of the absorbed power distribution between the suspended graphene and the trench. To verify that there is no strong thermal coupling between graphene and SiO_2 layer, we determined the positions of W_2 and W_3 Si–O–Si stretching bonds[25,26] in the range of 800–1100 cm^{-1} at different power levels. The absence of shifts suggests that SiO_2 layer is not heated despite its low K (~1 W/m K).

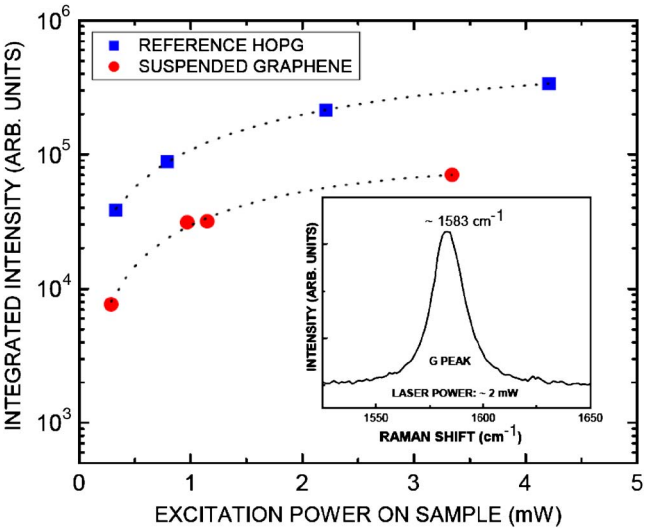

FIG. 2. (Color online) Integrated Raman intensity for the spectra region near G peak for suspended graphene and reference HOPG sample. The intensity ratio is approximately constant over the relevant excitation power range. Inset show the G peak region for graphene.

Figure 3 shows a change in the G peak position with the total dissipated power P_D for a typical suspended SLG. In this figure, the peak position change $\Delta\omega$ is referenced to the value at the lowest excitation power. The extracted slope is $\Delta\omega/\Delta P_D\approx-1.226$ cm^{-1}/mW. Knowing $\varsigma=\Delta I_G/\Delta I_{HOPG}$ for

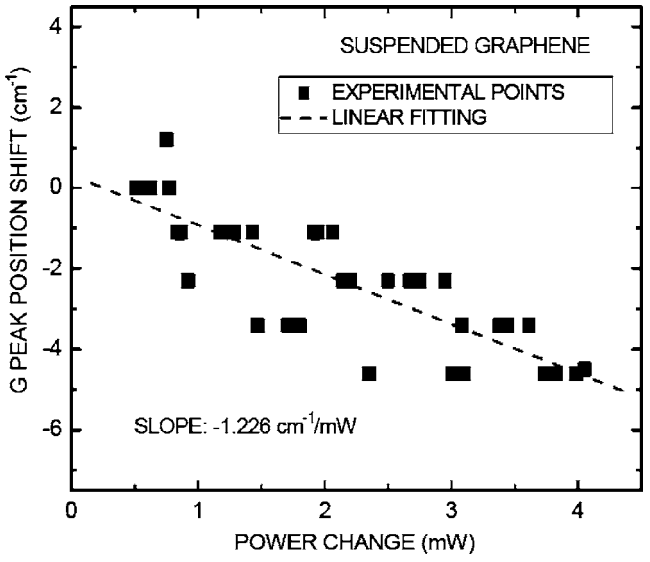

FIG. 3. The shift in G peak spectral position vs change in total dissipated power. The slope of the dependence is used for the extraction of the thermal conductivity of graphene.

a given sample and power range, one can recalculate the measured slope into the value of $\Delta\omega/\Delta P_G$. Using $\chi_G=-1.6\times10^{-2}$ cm^{-1}/K (Ref. 17) and plugging into Eq. (1) the values of a_G, L, and $\Delta\omega/\Delta P_G$, we obtain, for the examined set of SLG samples, the averaged values in the range of $K\sim3080-5150$ W/m K. One should note that the upper bound of K for graphene is higher than the conventionally accepted values for individual CNTs.[5,6] The standard error in our measurement of $\Delta\omega/\Delta P_D$ is ~9%.

From the Wiedemann–Franz law $K_e/\sigma=(\pi^2/3)(k_B/e)^2T$ (where K_e is the electron contribution to K, $\sigma=1/\rho$ is the electrical conductivity, ρ is the electrical resistivity, k_B is the Boltzmann constant, and e is the charge of an electron) and the measured resistance $R=\rho L/S\sim1$ kΩ for the graphene conductor of the length L and cross-sectional area S, we estimated that the contribution of electrons to the thermal conductivity is less than 1% at RT. This may seem unusual for a semimetal but in line with the predictions for graphite.[27] We evaluated the phonon MFP Λ in graphene from the expression $K=(1/2)CV\Lambda$, where C is the specific heat and V is the averaged phonon velocity. The coefficient 1/2 appears due to the two-dimensional nature of SLG. Using similarity of graphene and CNT material parameters and the data provided in Ref. 18, we estimated from our K values that MFP in graphene is $\Lambda\sim775$ nm near RT.

The Umklapp-limited phonon thermal conductivity can be approximated as $K=\rho V^4/(T\gamma^2\omega_D)$,[27,28] where ρ is the mass density, γ is the Gruneisen parameter, and ω_D is the Debye cutoff frequency. In order to get a rough estimate for K of graphene as compared to that of CNTs, K_{CNT}, we neglect the difference in ρ and ω_D, and write: $K/K_{\mathrm{CNT}}\approx(V_G/V_{\mathrm{CNT}})^4(\gamma_{\mathrm{CNT}}/\gamma_G)^2$. There is a discrepancy in reported values of γ for graphitic materials. At the same time, the published data suggest that γ for graphene is smaller than that in graphite or CNTs. Using the values for graphene from Ref. 29 and CNTs from Ref. 30, one gets $(\gamma_{\mathrm{CNT}}/\gamma_G)^2\approx1.37$. Thus, if one assumes equal phonon velocities in CNTs and graphene, the thermal conductivity of graphene should be larger than that in CNTs. For K_{CNT} values reported in Refs. 5 and 6 we would get graphene's low bound K estimate of ~4100–4800 W/m K. It has been suggested that the in-plane Gruneisen parameter of graphite reduces with increasing temperature near RT.[31] The latter can be a possible reason for the higher maximum value obtained in our experiment because graphene flakes experience substantial temperature rise. Based on the dispersion calculations in graphitic materials,[32,33] the phonon group velocity in graphene is higher than that in CNTs, which leads to larger K.

An important implication of extremely high thermal conductivity of graphene is its possible use for thermal management in future ULSI circuits. While SLG is hard to produce, graphene multilayers are much cheaper and are expected to retain the heat conducting property. Graphene layers can be naturally attached to heat sinks, thus, avoiding the problem of thermal contact resistance, which is a major issue for CNTs. The flat plane geometry of graphene simplifies its integration with Si CMOS circuits for thermal management.

The work of A.A.B. group was supported by DARPA-SRC through the FCRP Center on Functional Engineered Nano Architectonics (FENA). The work of C.N.L. and A.A.B. groups was supported, in part, by DARPA-DMEA through the UCR—UCLA—UCSB Center for Nanoscience Innovations for Defense (CNID). A.A.B. acknowledges useful discussions with Dr. A. C. Ferrari, Dr. P. Kim, Dr. R. Lake, Dr. K. L. Wang, and Dr. D. G. Cahill.

[1] A. Vassighi and M. Sachdev, *Thermal and Power Management of Integrated Circuits* (Springer, New York, 2006).
[2] S. Jin and H. Mavoori, J. Electron. Mater. **27**, 1148 (1998).
[3] M. J. Biercuk, M. C. Llaguno, M. Radosavljevic, J. K. Hyun, and A. T. Johnson, Appl. Phys. Lett. **80**, 2767 (2002); S. T. Huxtable, D. G. Cahill, S. Shenogin, L. Xue, R. Ozisik, P. Barone, M. Usrey, M. S. Strano, G. Siddons, M. Shim, and P. Keblinski, Nat. Mater. **2**, 731 (2003).
[4] A. V. Sukhadolou, E. V. Ivakin, V. G. Ralchenko, A. V. Khomich, A. V. Vlasov, and A. F. Popovich, Diamond Relat. Mater. **14**, 589 (2005).
[5] P. Kim, L. Shi, A. Majumdar, and P. L. McEuen, Phys. Rev. Lett. **87**, 215502 (2001).
[6] E. Pop, D. Mann, Q. Wang, K. Goodson, and H. Dai, Nano Lett. **6**, 96 (2006).
[7] K. S. Novoselov, A. K. Geim, S. V. Morozov, D. Jiang, Y. Zhang, S. V. Dubonos, I. V. Grigorieva, and A. A. Firsov, Science **306**, 666 (2004).
[8] Y. B. Zhang, Y. W. Tan, H. L. Stormer, and P. Kim, Nature (London) **438**, 201 (2005).
[9] A. K. Geim and K. S. Novoselov, Nat. Mater. **6**, 183 (2007).
[10] F. Miao, S. Wijeratne, Y. Zhang, U. C. Coskun, W. Bao, and C. N. Lau, Science **317**, 1530 (2007).
[11] A. C. Ferrari, J. C. Meyer, V. Scardaci, C. Casiraghi, M. Lazzeri, F. Mauri, P. Piscanec, D. Jiang, K. S. Novoselov, S. Roth, and A. K. Geim, Phys. Rev. Lett. **97**, 187401 (2006).
[12] I. Calizo, F. Miao, W. Bao, C. N. Lau, and A. A. Balandin, Appl. Phys. Lett. **91**, 071913 (2007).
[13] I. Calizo, W. Bao, F. Miao, C. N. Lau, and A. A. Balandin, Appl. Phys. Lett. **91**, 201904 (2007).
[14] I. Calizo, D. Teweldebrhan, W. Bao, F. Miao, C. N. Lau, and A. A. Balandin, J. Phys. C (unpublished).
[15] M. Kuball, S. Rajasingam, A. Sarua, M. J. Uren, T. Martin, B. T. Hughes, K. P. Hilton, and R. S. Balmer, Appl. Phys. Lett. **82**, 124 (2003).
[16] A. A. Balandin, S. Ghosh, W. Bao, I. Calizo, D. Teweldebrhan, F. Miao, and C. N. Lau, Nano Lett. **8**, 902 (2008).
[17] I. Calizo, A. A. Balandin, W. Bao, F. Miao, and C. N. Lau, Nano Lett. **7**, 2645 (2007).
[18] C. H. Yu, L. Shi, Z. Yao, D. Y. Li, and A. Majumdar, Nano Lett. **5**, 1842 (2005).
[19] H. Y. Chiu, V. V. Deshpande, H. W. C. Postma, C. N. Lau, C. Miko, L. Forro, and M. Bockrath, Phys. Rev. Lett. **95**, 226101 (2005).
[20] P. Blake, E. W. Hill, A. H. Castro Neto, K. S. Novoselov, D. Jiang, R. Yang, T. J. Booth, A. K. Geim, and E. W. Hill, Appl. Phys. Lett. **91**, 063124 (2007).
[21] M. C. Tobin, *Laser Raman Spectroscopy* (Wiley-Interscience, Toronto, 1971); M. M. Sushchinskii, *Raman Spectra of Molecules and Crystals* (Nauka, Moscow, 1969).
[22] A. Pfrang and Th. Schimmel, Surf. Interface Anal. **36**, 184 (2004).
[23] S. Perichon, V. Lysenko, B. Remaki, and D. J. Barbier, J. Appl. Phys. **86**, 4700 (1999).
[24] R. Tsu and J. G. Hernandez, Appl. Phys. Lett. **41**, 1016 (1982).
[25] F. L. Galeener, Phys. Rev. B **19**, 4292 (1979); A. E. Geissberger and F. L. Galeener, *ibid.* **28**, 3266 (1983).
[26] R. J. Hemley, H. K. Mao, P. M. Bell, and B. O. Mysen, Phys. Rev. Lett. **57**, 747 (1986).
[27] P. G. Klemens and D. F. Pedraza, Carbon **32**, 735 (1994).
[28] R. Gaume, B. Viana, D. Vivien, J.-P. Roger, and D. Fournier, Appl. Phys. Lett. **83**, 1355 (2003).
[29] M. Hanfland, H. Besister, and K. Syassen, Phys. Rev. B **39**, 12598 (1989).
[30] S. Reich, H. Jantoljak, and C. Thomsen, Phys. Rev. B **61**, 13389 (2000).
[31] N. A. Abdulaev, R. A. Suleimanov, M. A. Aldzhanov, and L. N. Alieva, Phys. Solid State **44**, 1859 (2002); N. A. Abdulaev, *ibid.* **43**, 727 (2001).
[32] M. S. Dresselhaus and P. C. Eklund, Adv. Phys. **49**, 705 (2000).
[33] N. Mounet and N. Marzari, Phys. Rev. B **71**, 205214 (2005).